

Electrical Resistivity Measurement with NI USB-6255 Data Acquisition Device

¹Okoh H., ²Azi S.O. and ²Ikhifa I.

¹Department of Physics, College of Physical Education, Mosogar, Delta State, Nigeria

²Department of Physics, University of Benin, Benin City, Nigeria

Abstract

One of the challenges of developing nations is the dearth of measurement devices. Aside the shortage, available equipments are obsolete and new ones are very expensive. When this is the situation, researchers must then design alternative methods to enable them carry out their experiments. The conventional terrameters are robust earth resistivity measuring equipments but are unavailable in many universities. A popular example is the ABEM 1000 and 4000 series. These devices come with a very high starting price of 50,000 US dollars depending on its capability. Geophysics students/researchers can barely go for field studies because of dearth of these equipments and modest efforts by researchers to design terrameters have not been very popular. Resistivity is traditionally measured with ammeters for current and voltmeters for potentials. Recently, computer-aided measurement and automation have replaced traditional instruments which now resulted in virtual instrumentation that mimics the appearance of traditional devices. This project focuses on design of virtual instrument (VI) system for electrical resistivity survey in Schlumberger. VI system is cheap, flexible, cost-effective, makes it easy to record full waveforms in real time, measurement is effective, user-friendly and can be modified for many different applications. The VI system comprises PC for display, signal generator for ac current, DAQ for voltage and current measurement.

The VI system comprises of personal computer for display, signal generator for ac current, data acquisition (DAQ) device for voltage and current measurement.

The interpreted results of this survey showed a noticeable level of consistency in the calculated percentage error for both VI and ABEM terrameter SAS 4000 respectively. The VI showed a percentage error of 6.18% whereas ABEM revealed a percentage error of 3.63% which is indicative of the fact that the VI system is a good earth resistivity measurement device. The results obtained from both VI and ABEM terrameter revealed a close semblance.

Keywords: Cost-effective, Data acquisition (DAQ), Full-waveform, Multi-disciplinary, Schlumberger array, Virtual Instrumentation (VI).

1.0 Introduction

The starting point of any geophysical investigation must be basic physics. Geophysics will only be effective if a target of interest has a physical contrast with the surrounding ground [1]. The application of the study of principles of physics to the study of geophysics yields a discipline in which several basic concepts of physics can be integrated to a single area of study. The cross-disciplinary field of geophysics makes it possible for many such applications of physics theories to real-world situations. In order to develop a technique for geophysical investigations, an instrumentation system capable of acquiring accurate data, analysis and presenting the data is important [2].

It is well known that geophysical equipments are expensive, rugged and reliable. It is not surprising therefore to find that many higher institutions of learning and research institutes, in a developing economy like ours, lack these equipments. Particularly, the handy terrameter for electrical resistivity measurements. A humble attempt has been made in this study to draw on the electronic resources of modern data acquisition systems and a laptop with usual electrode configurations for resistivity measurements. The thrust of the study brings to bear on fundamental principles of instrumentation, rapid data acquisition, signal processing and electrical noise in the earth. The instrument affords the student an opportunity to examine in fine details the way earth modifies a signal probe – which is the essence of geophysics.

The study of earth resistivity with virtual instrument system is a recent development. Virtual instrumentation is an interdisciplinary field that merges sensing, hardware and software technologies in order to create flexible and sophisticated instruments for control and monitoring applications [3]. The main philosophy behind the invention of the

Corresponding author: Okoh H.E-mail: okoh_henry1@yahoo.com, Tel.: +2348037201294

virtual instruments is to develop a powerful, yet flexible and cost effective instrumentation system that is using a standard personal computer and affordable software [4].

2.0 Theory

In terms of electromagnetic field quantities, consider an electric field E (volts/m) with current density J (amps/m²) and resistivity, ρ (Ωm). The vector form of Ohm’s law can be written as:

$$E = \rho J, J = \frac{E}{\rho} = \frac{I}{A} = \sigma E = \frac{-1}{\rho} \nabla V \tag{1}$$

Where

V = electric potential in volts and σ = conductivity measured in (Ωm)⁻¹.

We are interested in voltage at a distance ‘r’ from a point source of current in a half-space and not a whole space bearing in mind the air over the half-space. Again, we do not measure potential, but determine the potential difference between two electrodes. For a whole space, the total current I, flow away from one electrode to another across the sphere with area 4πr². Ohm’s law for one electrode then becomes

$$j = \frac{I}{4\pi r^2} = \frac{-1}{\rho} \cdot \frac{dV}{dr} \tag{2}$$

Integrating, we get

$$\frac{I}{4\pi r^2} \int dr = \frac{-1}{\rho} \int dV \tag{3}$$

$$\frac{I}{4\pi} \int r^{-2} dr = \frac{-1}{\rho} \int dV \tag{4}$$

$$\frac{-I}{4\pi r^1} = \frac{-1}{\rho} V(r) \tag{5}$$

$$V(r) = \frac{\rho I}{4\pi r} \tag{6}$$

But for a half-space, the total current (I), flows across the sphere with area ½(4πr²). So, V(r) becomes

$$V(r) = \frac{\rho I}{2\pi r} \tag{7}$$

I = total current flowing from one current electrode to the other through the ground.

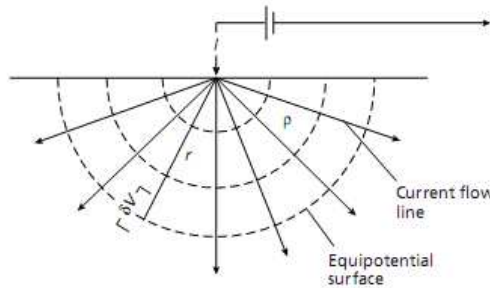


Figure 1: Distribution of current flow in a homogeneous soil [5]

However, the potential and current electrodes are usually arranged in a collinear pattern as shown in Figure 1. The distance between a current and potential electrode is denoted by r_{ij} where the first subscript denotes the current electrode(C) and the second, potential electrode (P). The electric potentials measured at M and N in the general linear arrangement (Figure 2) is a superposition of equation (7) due to each source electrodes located at A and B. The distances between the electrodes are given by AM, BM, AN, and BN. V = 0 infinitely far from the current source, the potentials at M and N can thus be calculated using equation (7).

$$V_M = \frac{\rho I}{2\pi} \left[\frac{1}{r_{AM}} - \frac{1}{r_{BM}} \right] \tag{8}$$

Note the minus sign because of the current convention. We also have that

$$V_N = \frac{\rho I}{2\pi} \left[\frac{1}{r_{AN}} - \frac{1}{r_{BN}} \right] \tag{9}$$

The thrust of this research is measuring the voltage drop, ΔV between two electrodes, M and N.

The potential ΔV may be measured as

$$\Delta V = V_M - V_N \tag{10}$$

Putting equation (8) and (9) together gives (11)

$$\Delta V = \frac{\rho I}{2\pi} \left[\frac{1}{r_{AM}} - \frac{1}{r_{BM}} - \left(\frac{1}{r_{AN}} - \frac{1}{r_{BN}} \right) \right] \tag{11}$$

$$\Delta V = \frac{\rho I}{2\pi} \left[\frac{1}{r_{AM}} - \frac{1}{r_{BM}} - \frac{1}{r_{AN}} + \frac{1}{r_{BN}} \right] \tag{12}$$

$$\Delta V = \frac{\rho I}{2\pi} \left[\frac{1}{r_{AM}} + \frac{1}{r_{BN}} - \frac{1}{r_{BM}} - \frac{1}{r_{AN}} \right] \tag{13}$$

By solving equation (13) for ρ, we can determine the resistivity of the subsurface region. Equation (13) was derived by assuming a homogeneous and isotropic half-space. Because we are dealing with a heterogeneous earth, a measured

voltage drop yields a resistivity value that is a weighted average along the current path way. Now, one can only consider apparent resistivity ρ_a of the subsurface.

$$\rho_a = 2\pi \frac{\Delta V}{I} \left[\frac{1}{r_{AM}} + \frac{1}{r_{BN}} - \frac{1}{r_{BM}} - \frac{1}{r_{AN}} \right]^{-1} \tag{14}$$

$$\rho_a = \frac{\Delta V}{I} K \tag{15}$$

$$\rho_a = R_{app} \cdot K \tag{16}$$

Where $K = 2\pi \left[\frac{1}{r_{AM}} + \frac{1}{r_{BN}} - \frac{1}{r_{BM}} - \frac{1}{r_{AN}} \right]^{-1}$ (17)

K is the “geometric factor” that will obtain a certain value for a given electrode configuration. For the wenner array, all of the separations are equal to a constant value “a” [6].

In the schlumberger array, the current electrodes, separated by AB are symmetrical about the potential electrodes, MN. The current electrodes are then expanded and the geometric factor K assumes the form

$$K = \frac{\pi}{2} \cdot \frac{\left(\frac{AB}{2}\right)^2 - \left(\frac{MN}{2}\right)^2}{\left(\frac{MN}{2}\right)} \tag{18}$$

Putting equation (18) into (15), the apparent resistivity for the Schlumberger array becomes

$$\rho_a = \frac{\Delta V}{I} K = \frac{\pi}{2} \cdot \frac{\left(\frac{AB}{2}\right)^2 - \left(\frac{MN}{2}\right)^2}{\left(\frac{MN}{2}\right)} \cdot \frac{\Delta V}{I} \tag{19}$$

Resistivity can be found from measuring values of V, I and K.

3.0 Materials/Methodology

The VI measurement system is in two parts – hardware and software as shown in Figure 2.

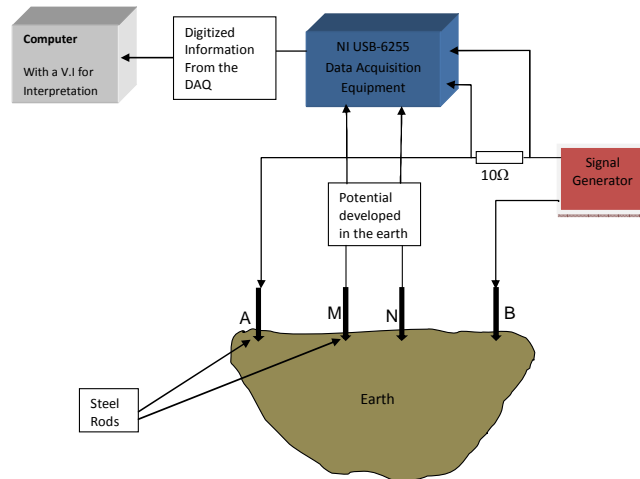


Figure 2: A typical PC-based DAQ system for earth resistivity survey

3.1 Hardware

The signal generator used is the manually controlled Harris Power Signal Generator. There are three types of pulse shape (triangular, square and sine) available and can generate a frequency range of 0.1Hz-2240Hz. The data acquisition is based on 96 channel 16bits NI USB-6255 analog to digital conversion ADC. The PC displays the signals on the screen.

3.2 Software

In a measurement system, the entire architecture cannot interface with the human user without software not to mention the fact that it is almost insignificant with inappropriate software. The software in this design is in two parts – The driver (NI-DAQ_{max}) and the application (LabVIEW SignalExpress). The NI-DAQ_{max} establishes communication between DAQ devices and the PCs. The LabVIEW SignalExpress is an interactive framework for measurement and automation. It is used for acquiring, analyzing, and presenting data from hundreds of acquisition devices and instruments, with no programming required [7].

4.0 Methodology

The whole set up was switched on after all the necessary arrangements of the signal generator, NI USB-6255, cables, and electrodes. Another aspect of the set-up is the installation of bias resistors of 10MΩ on both the current (ai0) and potential (ai1) channels as shown in Fig. 3. Vertical Electrical Sounding of the earth was performed using the NI USB-

6255 DAQ and the conventional ABEM terrameter for comparison. Measurement was done in Schlumberger array with half current electrode spacing varying from 1m to 100m. A signal of frequency 0.9Hz was generated from the signal generator. The square wave pulse generated was passed through a 10Ω resistor so as to enable calculation of the value of current going into the ground via current electrodes, A and B. The potential across the 10Ω resistor and the potential response across M and N from the subsurface were measured using the DAQ. The signals acquired were then transmitted to the PC via a USB cable for display. Sample of test records, filtered waveforms and calculated RMS values are as shown in Figs. 4 and 5.

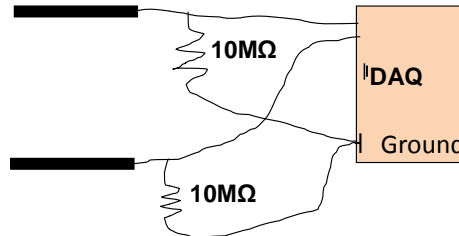


Figure 3: Bias resistors to reduce noise in potential measured between two electrodes [8]

5.0 Data Processing

Earth signals are however influenced by noise systems of varying frequencies from the environment. To further eliminate some of these unwanted frequency components, a post-acquisition processing was done. Filtering was performed in the LabVIEW SignalExpress GUI using a 4th order Butterworth low pass filter with a cut-off frequency of 5Hz. In the field of geophysics, noise cancellation is very essential to sustaining signal quality. Noise usually cannot be completely eliminated but can only be minimized to the point where it has little or no effect on measurement integrity. However, solutions to noise problems are usually found by trial and error with little understanding of the mechanisms involved [9].

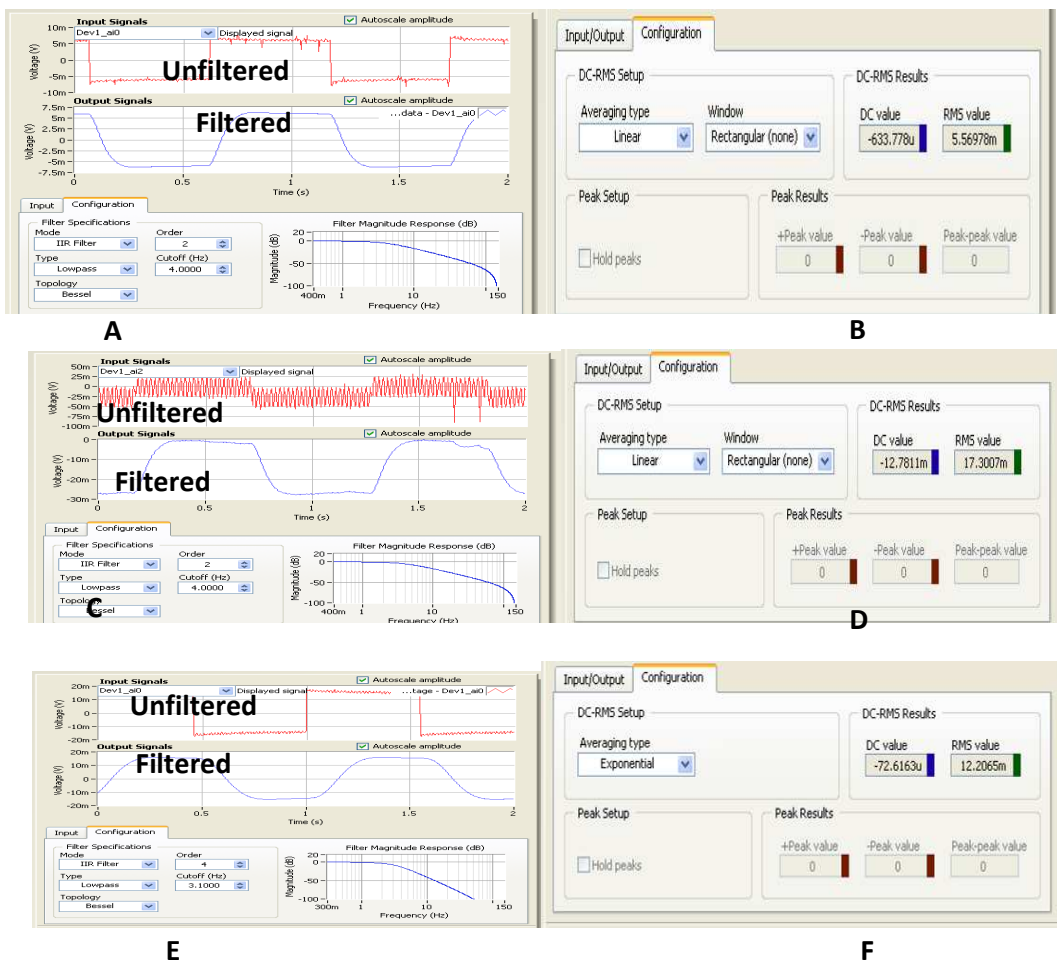


Fig. 4. Sample of VI test record: (A) Unfiltered and filtered signals for AB/2 = 3.16m(B) Amplitude and Levels step calculation to obtain potential value for AB/2 = 3.16m (C) Unfiltered and filtered signals for MN/2 = 0.5m (D) Amplitude and levels step calculation to obtain potential for MN/2 = 0.5m

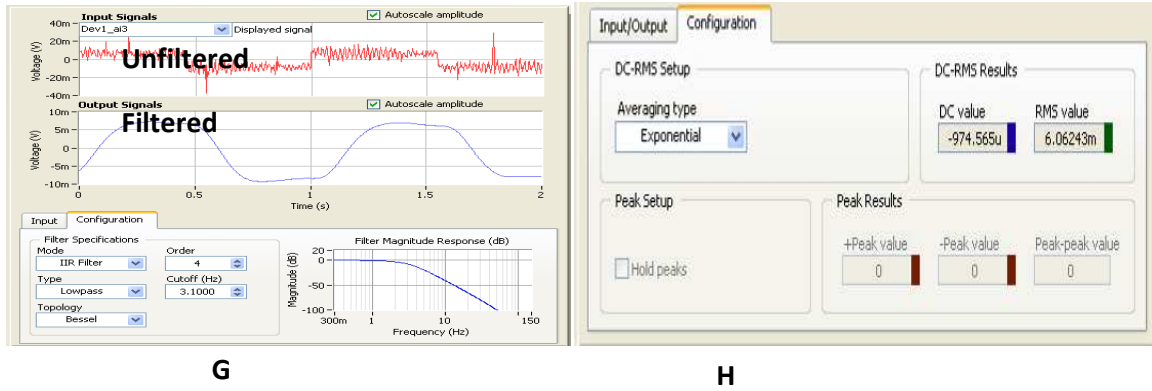


Fig. 5. Sample of VI test record: (E) Unfiltered and filtered signals for AB/2 = 100m (F) Amplitude and levels step calculation to obtain potential for AB/2 = 100m (G) Unfiltered and filtered signals for MN/2 = 20m (H) Amplitude and levels step calculation to obtain potential for MN/2 = 20m
The RMS value seen in levels and amplitude calculation dialog box was used to calculate true potential using equation (20).

$$V_{r.m.s} = \frac{V_0}{\sqrt{2}} \tag{20}$$

6.0 Data Analysis

LabVIEW SignalExpress program was used to perform amplitude and levels step measurement on the acquired signals. Since current was not measured directly, the potential measured across the 10Ω resistor was analyzed and the result divided by 10Ω 1% precision to derive a value of the current (Ohms law, V = IR) going into the ground. In the same vain, the potential response across MN electrodes was divided by value of current passed into the ground in order to obtain the value for resistance of the subsurface. This was done for all the AB spacing covered.

7.0 Results and Discussion

Apparent resistivity (ρ_a) was determined by multiplying the resistance values obtained with the geometric factor (K). K is a function of the array used and the arrangement of the four electrodes. The results of the apparent resistivity (ρ_a) values for AB/2 = 1m and AB/2 = 100m formed the basis of comparison between the VI system and the ABEM terrameter. The apparent resistivity values obtained for both the VI and ABEM are as shown in Table 1.

Table 1: Apparent resistivity values for both VI and ABEM terrameter

S/N	AB/2 (m)	VI ρ_a (Ωm)	ABEM ρ_a (Ωm)
1	1.00	409.52	415.07
2	1.47	534.04	587.12
3	2.15	799.50	753.82
4	3.16	950.15	944.38
5	4.64	1193.14	1002.07
6	6.81	1163.53	1137.00
7	10.00	1112.04	1282.16
8	14.70	1296.92	1221.18
9	21.50	1374.36	1335.18
10	31.60	1471.29	1826.88
11	46.40	2254.23	2412.90
12	68.10	3355.24	3314.22
13	100.00	3745.18	3940.82

The vertical electrical sounding data were then interpreted using the IPI2Win software program. This interpretation was done to obtain the true resistivity of the layers in the subsurface. The sounding curves show geoelectrical layers of various resistivities and thicknesses as presented in Figs. 6 and 7 and also Table 2.

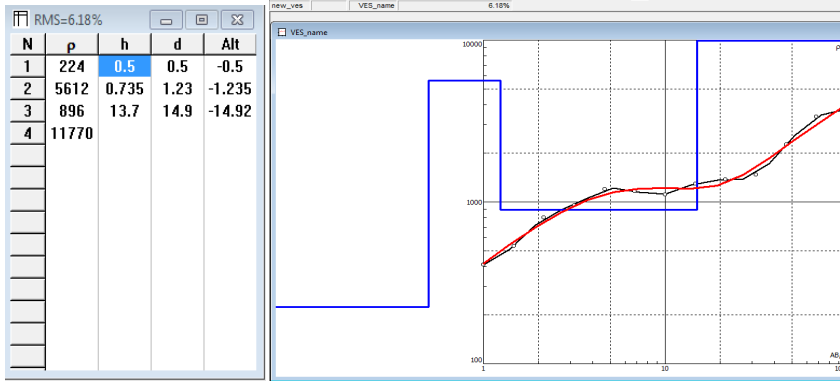


Fig. 6. IPI2Win plot of apparent resistivity (ρ_a) against AB/2 spacing for VI (UNIBEN)

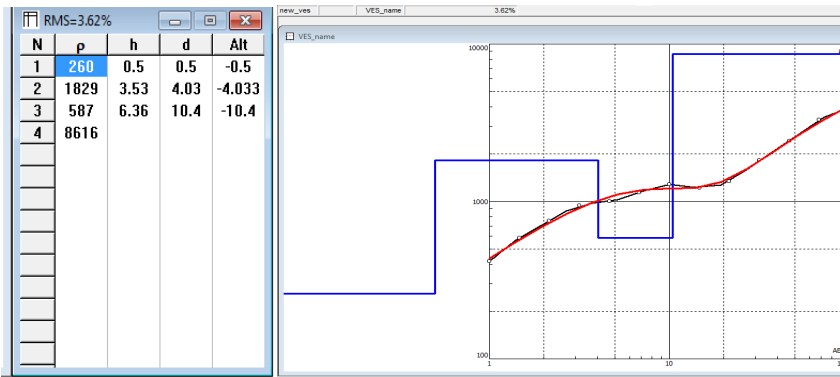


Fig. 7. IPI2Win plot of apparent resistivity (ρ_a) against AB/2 spacing for ABEM terrameterSAS 4000 (UNIBEN)

In Fig. 6, the VES curves show a KH ($\rho_1 < \rho_2 > \rho_3 < \rho_4$) curve type whereas Fig. 7 presents VES curves with KH ($\rho_1 < \rho_2 > \rho_3 < \rho_4$) type curve which also confirms the similarity of results between VI and ABEM terrameter SAS 4000. The IPI2Win software automatically performs interpretation on the 1-dimensional apparent resistivity data and generates the model parameters without any human control. This is the much reason why it is possible to have different models representing six layers at a certain location and may be five layers at other locations. A summary of results showing root-mean-square (RMS) error, number of geoelectrical layers, resistivity values, thicknesses and depths of various layers are in Table 2.

Table 2:Summary of VES results for both VI and ABEM terrameter

VES NO	SOUNDING RMS ERROR	GEOELECTRICAL LAYERS	RESISTIVITY (Ω m)	THICKNESS (m)	DEPTH (m)
1(DAQ)	6.18%	1	224.00	0.50	0.50
		2	5612.00	0.73	1.23
		3	896.00	13.70	14.90
		4	11770.00	-	-
2(ABEM)	3.62%	1	260.00	0.50	0.50
		2	1829.00	3.53	4.03
		3	587.00	6.36	10.40
		4	8616.00	-	-

A fit between the measured data and the calculated data is very good with less than 10% for both VI and ABEM terrameter. Four layers of different resistivities were also detected.

In case of the VI, the VES model shows four layers with resistivities of 224 Ω m, 5612 Ω m, 896 Ω m and 11770 Ω m respectively. The first layer has resistivity of 224 Ω m representing the topsoil. The second and third layers have resistivity range of between 5612 Ω m to 896 Ω m representing brown sand. The VES model for the ABEM terrameter SAS 4000 also revealed four layers with resistivities of 260 Ω m, 1829 Ω m, 587 Ω m and 8616 Ω m. Similarly, the first layer has resistivity of 260 Ω m representing the topsoil. Just as in the case of VI, the second and third layers have resistivities ranging from 1829 Ω m to 587 Ω m signifying brown sand. However, the depths and thicknesses of the 4th layer for both the VI and ABEM terrameter SAS 4000 were not captured. This is probably due to the fact that current did not penetrate through this layer. Interpretation of the VES data obtained for both the DAQ and ABEM terrameter SAS 4000 revealed four similar resistivity values as shown in Table 2.

8.0 Conclusion

By carrying out earth resistivity measurements in schlumberger array with both the VI system and the conventional ABEM terrameter, it was possible to show that both operated closely together. The following conclusions can be drawn from the test carried out.

1. The VI and ABEM systems operated closely together at the same half current (AB/2) electrode spacing.
2. Full waveform monitoring was possible with the VI system but not with ABEM terrameter.
3. The VI system is user-defined and can be used for many different applications whereas the ABEM is manufacturer-defined and can only be used for resistivity measurements. The researcher has no control to expand or modify the existing functions unlike the VI system.
4. Signals acquired can be stored for future use and playback of pre-recorded signal is possible.
5. Selection of a signal pattern (square, triangular or sine) of choice was possible in the VI system.

References

[1] Johnson, J.W. Applications of the electrical resistivity method for detection of underground mine workings: Underground coal mine voids, Lexington, KY, USA, July 2003.

[2] NGRI. Exploration, Assessment and Management of Groundwater Resources Annual Report 2008-2009 pp.72.[Online]Available:<http://www.ngr.org.in/export/sites/default/> (Assessed on May 13, 2014).

[3] ObrenovicŽ.,Starcevic D., JovanovE.Virtual Instrumentation, in Metin- Akay (Editor): Wiley Encyclopedia of Biomedical Engineering. ISBN: 0-471-24967-X, DOI: 10.1002/9780471740360.ebs1265; Wiley, pp. 2, 2006.

[4] Saoud H. S.Internet-Based Monitoring and Controlling of Real-Time Dynamic Systems, M. Sc., Thesis, Department of Electrical and Computer Engineering, Curtin University of Technology, Perth, Australia, 2005.

- [5] Kearey P., Brooks M., Hill I. (2002).An Introduction to Geophysical Exploration, Third Edition. Blackwell Science Publishing Ltd, pp30-32.
- [6] Herman, R. An introduction to electrical resistivity in geophysics: Department of chemistry and physics and department of geology, Radford University, Radford, Virginia 24142, USA, 2001.
- [7] National Instruments. National Instruments LabView SignalExpress: Getting Started with LabView SignalExpress. National Instruments Corporation, Austin, Texas, USA, 2008.
- [8] Forté, S. Mapping Organic Contaminant Plumes in Groundwater Using Spontaneous Potentials, Ph.D. Thesis, Department of Geoscience, University of Calgary, Alberta, Canada,pp. 132, 2011.
- [9] Pezeshkpour, P. Hydrogeological Application of Electrical Resistivity Tomography: Implementing a fixed – Electrode Strategy, Ph.D. Thesis, Dept. Earth Sciences, University of Waterloo, Ontario, Canada; pp. 57-61, 1999.